Elastomeric Domain-Type Interpenetrating Polymer Networks

M. S. SILVERSTEIN and M. NARKIS, *Department of Chemical Engineering, Technion City, Haifa 32000, Israel*

Synopsis

Elastomeric latex interpenetrating polymer networks (IPNs) can result from a two-stage emulsion polymerization procedure in which styrene is polymerized and cross-linked on a lightly cross-linked polyacrylate (PA) seed latex in a ratio of 75 : 25 PA-PS. The multiphase nature of these IPNs is indicated by two distinct T_gs and is confirmed by cold-stage transmission electron microscopy and by the unique mechanical and rheological properties that are intimately related to the material's structure. PS microdomains reinforce the elastomeric PA, yielding a significant modulus, and interparticle PS physical ties yield a significant ultimate tensile strength. The elastomeric latex IPN's dual thermoset-thermoplastic nature is revealed in a stick, slip, roll flow mechanism of the cross-linked submicrometer particles, which can be injection molded as a thermoplastic. The relationships among the polymerization procedure, the structure, and the physical properties are characterized by the examination of several different materials using a variety of analytic techniques.

INTRODUCTION

The behavior of a multiphase polymeric material can be understood through a thorough characterization procedure using mechanical, rheological, thermal, and electron microscopic techniques and a variety of other analyses. Multiphase polymers, two classic examples of which are styrene-butadiene-styrene (SBS) triblock copolymer thermoplastic elastomers and high-impact polystyrene (HIPS), result from incompatible or semi-incompatible blends, block copolymers, graft copolymers, and interpenetrating networks (IPNs).[1] The unusual properties of the thermoplastic SBS elastomers stem from the phase-separated glassy domains throughout the continuous elastomeric polybutadiene phase. These domains act as physical cross-links at room temperature but disintegrate at elevated temperatures, allowing the polymer to flow.[2,3] The energy absorption mechanism of crazing in HIPS stems from the presence of small rubbery particles dispersed in a continuous glassy matrix.[4,5] The behavior of these multiphase polymeric materials is affected by the composition, size, and structure of the domains, and both the extent and the mode of mixing are important factors that must be characterized, understood, and controlled.

Interpenetrating polymer networks can be distinguished from other multiphase materials through their bicontinuous structure[6,7] and have been classified by the polymerization procedure used as sequential, simultaneous, or semi IPNs.[8] Highly compatible polymers should form an IPN structure having two distinct interwoven networks on the molecular level. The two polymers in a sequential IPN are often incompatible to some extent, and

Journal of Applied Polymer Science, Vol. 33, 2529–2547 (1987)
 CCC 0021-8995/87/072529-19$04.00

phase separation, which may be incomplete owing to the structural constraints prevailing in a system in which a network is being formed within a swollen existing network, must be taken into consideration. The resolution attained with direct experimental techniques limits the characterization of these polymer structures, which may be of the order of hundreds of angstroms or less, and the establishment of their bicontinuous nature is not straightforward.[9]

A latex IPN may result from a sequential two-stage emulsion polymerization: the polymerization and cross-linking of monomer I followed by the polymerization and cross-linking of monomer II in the presence of the polymer I seed latex.[10,11] The parameters of the polymerization process, the hydrophilicity of the monomers, the compatibility of the polymers, the miscibility of polymer I in monomer II, and the degrees of cross-linking all play an important role in the determination of both the latex particle size and the particle's multiphase structure.[12,13] Four typical structures that can be produced through the manipulation of these parameters, for monomer II polymerized and cross-linked on a cross-linked seed latex of polymer I, are[3,14] a core of polymer I surrounded by a shell of polymer II (C/S); a core of polymer II surrounded by a shell of polymer I (inverted C/S); a matrix of polymer I with polymer II domains; and two continuous interwoven networks with or without the formation of some microdomains by partial phase separation. Small-angle neutron scattering has been used successfully to reveal the C/S structure of some two-stage latices,[15] and fluorescence techniques have revealed a microdomain structure in others.[16]

Two-stage emulsion polymerized IPNs composed of an elastomeric polymer, such as a polyacrylate (PA), and a glassy polymer, such as polystyrene (PS), yield materials of interest.[17] For a complete understanding of the IPN's behavior both the intraparticle and interparticle structures must be taken into account. At high PA concentrations the PS microdomains in the IPN can be compared to those in either SBS or filled elastomers, and at high PS concentrations the IPN can be compared to HIPS. Elastomeric latex IPNs consisting of soft polyacrylate and glassy polystyrene are the subject of this article.

EXPERIMENTAL

A standard semibatch emulsion polymerization procedure[18] was used to produce a cross-linked polymer I seed latex upon which the second stage was added in the same manner. A typical recipe is based on a seed latex comprising 30% poly(ethyl acrylate) (PEA) and 70% poly(butyl acrylate) (PBA) with 3% butadiene (BD) as a cross-linker. The second stage consists of styrene with 0.25% divinyl benzene (DVB) added as a cross-linker, with the ratio of monomer I to monomer II of 75 : 25. Variations in that recipe include the use of poly(ethyl hexyl acrylate) (PEHA) in the seed, ethylene glycol dimethacrylate (EGDMA) as the acrylate cross-linker, and methyl methacrylate and EGDMA as the second stage. The final two-stage polymer latex was coagulated and dried and could be compression or injection molded without further modification.

Both the high-temperature shear modification and the plasticization (using butyl benzyl phthalate, BBP, or dioctyl phthalate, DOP) of the material were accomplished using a roll mill or a Brabender mixing head. The static

mechanical properties at various temperatures were determined with an Instron tensile tester at a crosshead speed of 10 cm/min on 5 cm long dumbbell-shaped specimens that were injection or compression molded at 180°C. The rheological properties were examined with an Instron capillary rheometer, whose applied shear rate was varied from 0.05 to 500 s^{-1} through the variation of the plunger speed. Two series of dies were used, one of a constant diameter (1.3 mm) and varying lengths (25.4, 50.8, 76.2, and 101.6 mm) and the other of constant length (50.8 mm) and varying diameters (0.9, 1.3, 2.2, and 3.0 mm), at temperatures from 50 to 230°C.

The T_gs of the IPNs were determined through both dynamic mechanical spectroscopy (DMS) with a Rheometrics System 4 DMS in either torsion or parallel plate geometries, at low frequencies and strains, and differential

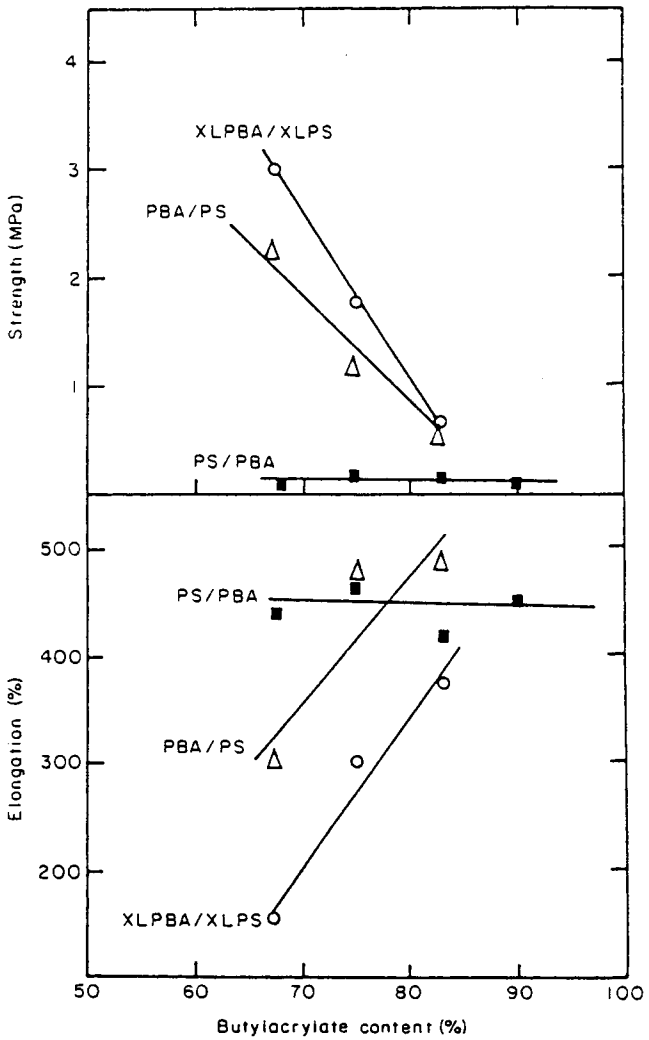

Fig. 1. Tensile properties of two-stage latex elastomers as a function of monomer sequence of addition, butyl acrylate content, and cross-linking. PS/PBA: butyl acrylate added to PS seed latex; PBA/PS: styrene added to PBA seed latex; XL: indicates that a cross-linker was added to the monomer.

scanning calorimetry (DSC) with a Mettler DSC operated at 10°C/min. The DMS parallel plate geometry was also used to study the dynamic viscosity of the IPN materials at low strains and temperatures above 100°C. The swelling of the IPN was examined in both pure solvents whose solubility parameters δ lay between 12 and 25 $(MJ/m^3)^{1/2}$, and mixtures of a pair of solvents with a δ at each end of the range. Polymer samples were loosely encased in a wire mesh envelope and placed overnight in a beaker filled with a solvent at room temperature. The samples were weighed while swollen with the solvent and after they had been dried in a vacuum oven for several hours.

Frozen latex specimens for transmission electron microscopy (TEM) were prepared by trapping a thin layer of diluted latex between two polyimide-covered electron microscope grids and plunging the "sandwich" into liquid nitrogen. The specimens were transferred into a JEOL JEM 100CX transmission electron microscope using a cold-stage transfer module (CSTM) and a modified JEOL cooling holder[19] and examined in the TEM with a 100-kV electron beam at 95 K. After selecting a suitable area at low magnification and low electron exposure (dose) rates, the magnification was increased to between ×10,000 and ×20,000 and the exposure rate was set at a predetermined value. Photographs were then taken at 30–60 s intervals with the beam left on, corresponding to a dose of 2–30 kC/m^2.

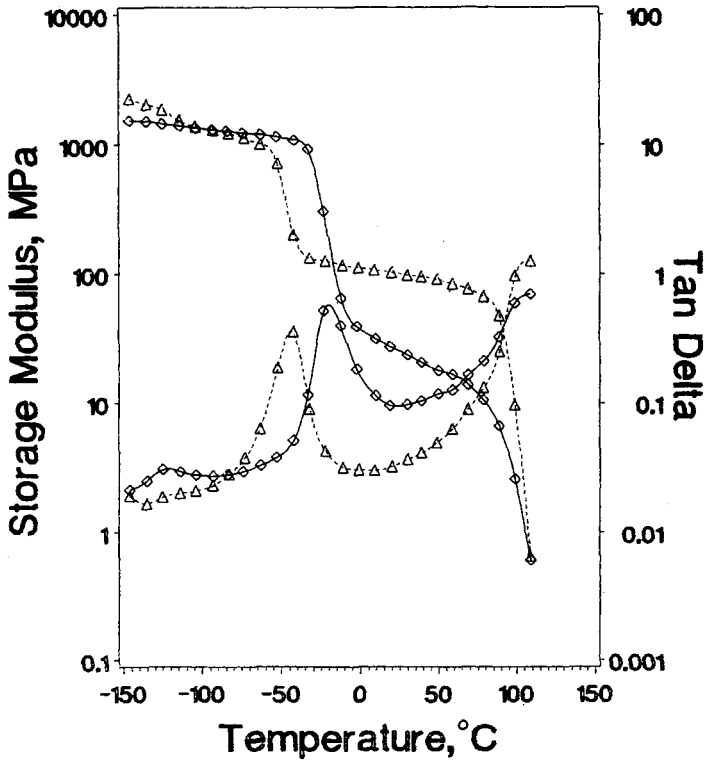

Fig. 2. DMS temperature sweep of IPNs in torsion at 6 Hz. (a) (---△---) 70:30 PA-PS; PA: BA, 1% EGDMA. (b) (—◇—) 75:25 PA-PS; PA: 85:15 EA-EHA, 3% BD + EGDMA. All PS cross-linked with 0.25% divinylbenzene.

RESULTS AND DISCUSSION

The Multiphase Structure

The various possible structures of two-stage latices can yield materials of the same composition with completely different properties, the sequence of the stages being a major factor in the determination of the particle structure. Polymers with PS as the seed latex yield very poor elastomers whose properties do not improve with the PS content, as seen in Figure 1, but polymers with PBA as the seed latex yield elastomers whose significant strength is dependent upon the PS content and the cross-linking. The strength-forming mechanism of the molded particles is dependent upon the interaction between them, and the weak links found in the PS-seeded materials indicate that the particles have a C/S structure with the PS cores as a filler in the PBA matrix. The PS core filled elastomeric particles have the coiled PBA molecules as their interparticle ties, yielding high elongation but extremely low tensile strength. The significant strength of the interparticle ties of the PA-seeded materials increases with the amount of PS, indicating the important part that the PS

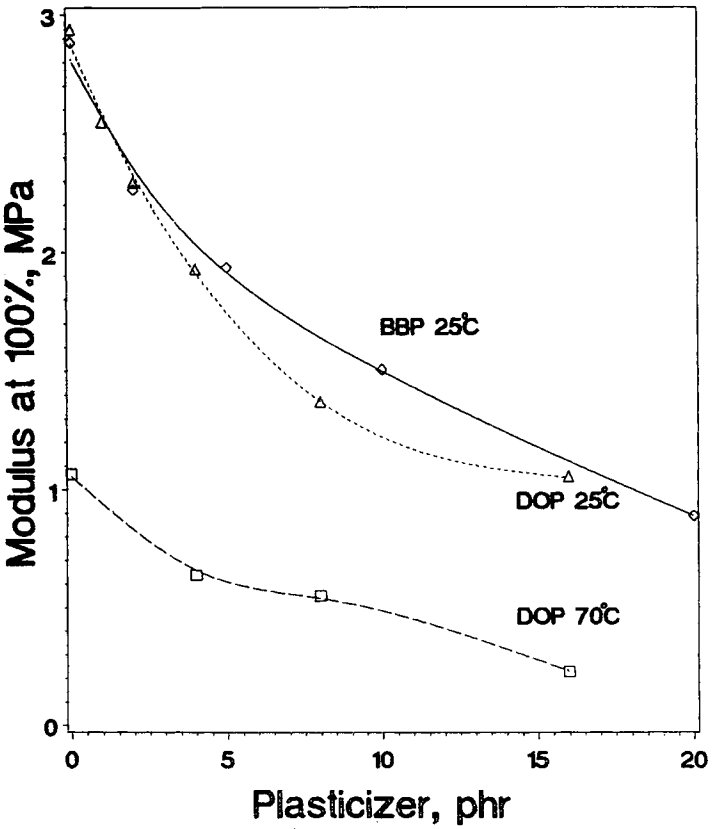

Fig. 3. Young's modulus at 100% of IPN of Figure 2b plasticized with butyl benzyl phthalate (BBP) and dioctyl phthalate (DOP): (a) (—◇—) BBP, 25° C. (b) (- - -△- - -) DOP, 25° C. (c) (– – □ – –) DOP, 70° C.

plays in holding the particles together and emphasizing the unique nature of these interparticle ties.

The significant modulus of the PA-seeded material, compared with the PS-seeded material, indicates that the largely elastomeric particles are highly reinforced by rigid PS domains, similar to the reinforcement of SBS. The shear storage modulus from the DMS studies in Figure 2 for two samples of different compositions and degrees of cross-linking supports this conclusion since the rubbery plateau between the two transitions is several orders of magnitude greater than those of cross-linked and filled cross-linked rubbers.[20] The plasticized IPN of Figure 2b exhibits a decrease in modulus with the increase in plasticizer concentration, as seen in Figure 3, behavior that can be linked to the effect of the plasticization on the reinforcing PS domains. The decrease in the modulus due to plasticization is greater at 25°C than at 70°C since at the higher temperature the reinforcing PS domains have already been softened. Thus in the PA-seeded materials the role of the PS, which has a significant influence upon both the tensile strength and the modulus, is much more than simply that of a filler.

Evaluation of the unplasticized IPN materials using DSC and DMS reveals two distinct T_gs, one between −50 and −20°C, depending on the composi-

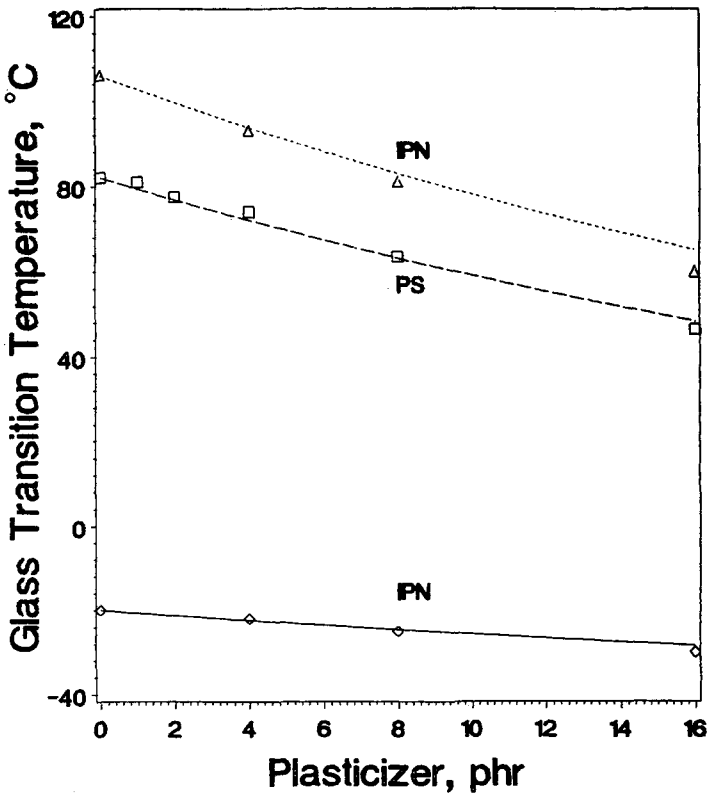

Fig. 4. Glass transition temperatures of PS and IPN of Figure 2b plasticized with dioctyl phthalate (DOP): (---△---) IPN, upper T_g; (—◇—) IPN, lower T_g; (– –□– –) PS. Symbols represent experimental points, lines generated using eq. (1).

tion of the polyacrylate seed, and one between 100 and 110°C, representing the PS domains. The DSC and DMS studies of these IPN materials, yielding almost identical results, have shown that the T_g of each phase in the DOP-plasticized IPN can be predicted using eq. (1),[21] with the T_g of DOP taken as −71°C. Figure 4 exhibits the decrease of the IPN's two T_gs with the addition of the plasticizer, and the accurate prediction of the experimental results by the lines generated using eq. (1) indicates that the plasticizer is apparently distributed evenly throughout the IPN rather than selectively absorbed by one of the phases. This nonselectivity, which might be of significance in similar but differently structured multiphase materials, could be due to the small size of the domains in the IPN. The decrease of 40°C in the upper T_g of the plasticized IPN at 16 phr is similar to that of pure PS, further supporting the evidence that the higher T_g represents PS domains.

$$\frac{1}{T_g} = \frac{w_1}{T_{g1}} + \frac{w_2}{T_{g2}} \tag{1}$$

where T_{gi} is the T_g of phase i, and w_i is the weight fraction of phase i.

The plasticizer has a significant influence on the IPN's mechanical and rheological properties mainly by affecting the higher T_g phase, the phase that

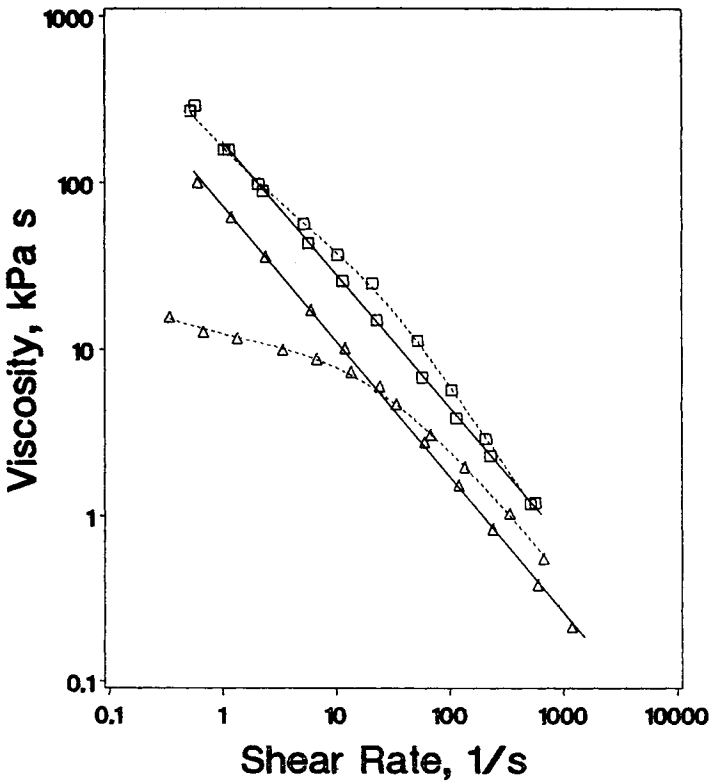

Fig. 5. Capillary rheometer flow curves of IPN of Figure 2b and SBS at various temperatures: □ 80°C; △ 150°C; (- - -) SBS; (—) IPN.

is important to both the interparticle interaction and the intraparticle reinforcing mechanism. The structure of these multiphase IPN materials combines interwoven bicontinuous networks in the particle structure, possibly with phase-separated reinforcing PS microdomains, with strengthening PS entanglements and domains acting as physical ties between the particles. This structure lends itself to further characterization owing to its unique combination of thermoset and thermoplastic properties.

Cross-Linked Latex Particles

The rheological properties of multiphase materials are a function of the structure and properties of the phases and their interaction. The flow behavior of SBS thermoplastic elastomers above 100°C, which exhibits a Newtonian plateau at low shear rates,[22] is not the same as that of carbon black-filled rubbers, which may exhibit a yield stress.[23-32] The elastomeric latex IPN is a multiphase material that might exhibit, in flow above 100°C at low shear rates, either a yield stress or a Newtonian plateau. Capillary rheometry studies on the elastomeric IPN materials[33] exhibit a power law behavior whose exponent is approximately 0.18 throughout the temperature range of 80–200°C. Neither a Newtonian plateau nor a yield stress were noted for the

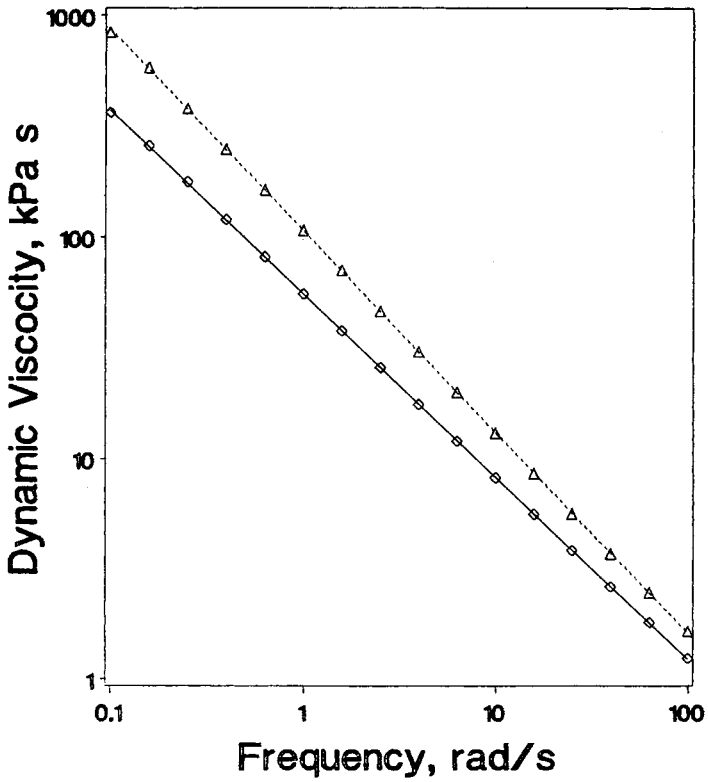

Fig. 6. DMS of IPNs of Figure 2 in rate sweep using parallel plate geometry at 150°C, 1% strain: (a) (- - - △ - - -) 70 : 30 PA-PS; PA: BA, 1% EGDMA. (b) (—◇—) 75 : 25 PA-PS; PA: 85 : 15 EA-EHA, 3% BD + EGDMA. All PS cross-linked with 0.25% divinylbenzene.

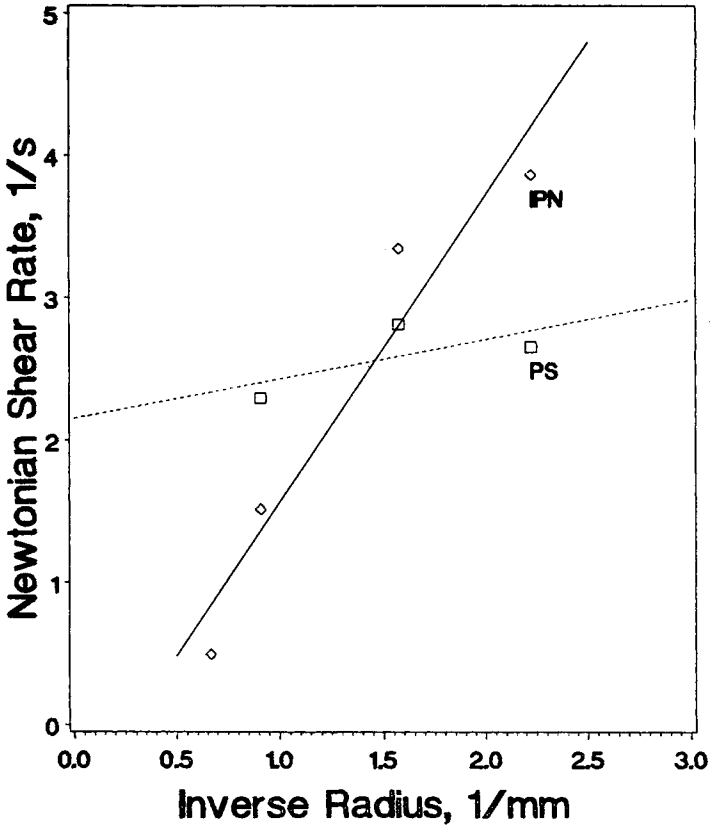

Fig. 7. Determination of slip velocity of the IPN of Figure 2b at the capillary rheometer wall: (—◇—) IPN; (- - -□- - -) PS.

IPN materials at the lowest shear rates studied. Comparison of the latex IPN with an SBS thermoplastic elastomer at 150 °C in Figure 5 demonstrates that the IPN continues to exhibit the same power law behavior throughout the shear rate range studied but the SBS develops a Newtonian plateau. The DMS parallel plate studies confirm the capillary rheometry analysis, as neither a Newtonian plateau nor a yield stress is evident at the low frequencies studied, as seen in Figure 6. The flow activation energies at constant shear stress of approximately 80 kJ/mol obey the relationship of eq. (2) derived from the power law and are of the same order of magnitude as standard thermoplastic materials.

$$E_{\dot{\gamma}} = nE_{\tau} \tag{2}$$

where: E_{τ} = activation energy at constant shear stress
$E_{\dot{\gamma}}$ = activation energy at constant shear rate
n = power law exponent

The rippling melt fracture of the extrudate found at all shear rates[33] indicates a stick, slip, roll flow mechanism similar to that proposed for rubbers and PVC.[34-40] The slip velocity at the wall at a constant shear stress and temperature, which is calculated using eq. (3) from the slope of Figure 7[41-43] is of the same magnitude as the Newtonian average velocity in shear for a given

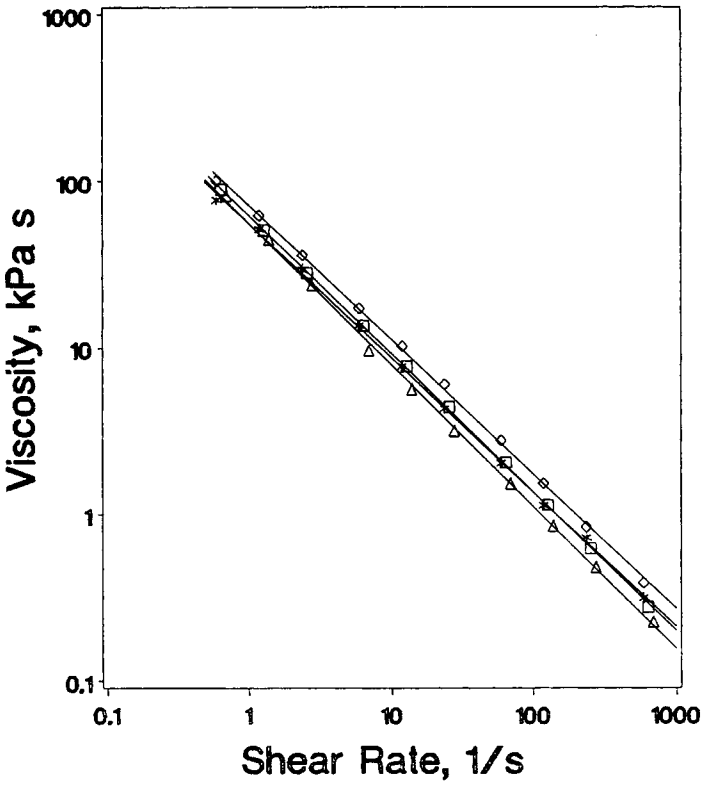

Fig. 8. Capillary rheometer flow curves at 150°C of roll-milled IPN of Figure 2b at various temperatures: ◇ untreated; △ 60°C; * 90°C; □ 150°C.

shear rate at the wall[44] and confirms the extent and importance of the stick and slip at the wall to the flow process. The flow units are presumably the lightly cross-linked, deformable, elastomeric, submicrometer latex particles connected by extendable, interchanging, physical "cross-links," similar to the basic assessment of the material's structure from the previous analyses.

$$\dot{\gamma}_w = \frac{4V_w}{R + K} \tag{3}$$

where: $\dot{\gamma}_w$ = shear rate at the wall
V_w = velocity at the wall
R = radius of the capillary
K = constant

The negligible effect of high-temperature roll mill shear modification on the latex IPN's flow behavior at 150°C, seen in Figure 8, confirms the structural stability of the deformable flow units, which regain their shape and level of interparticle interaction upon the cessation of shear. The flow units formed by the individual particles are more stable than those of PVC, which fuse irreversibly above 180°C and whose flow is greatly affected by plasticization.[21,45] The viscosity of the IPN was reduced with the addition of the plasticizer, as seen in Figure 9, more efficiently at 80°C than at 150°C, but

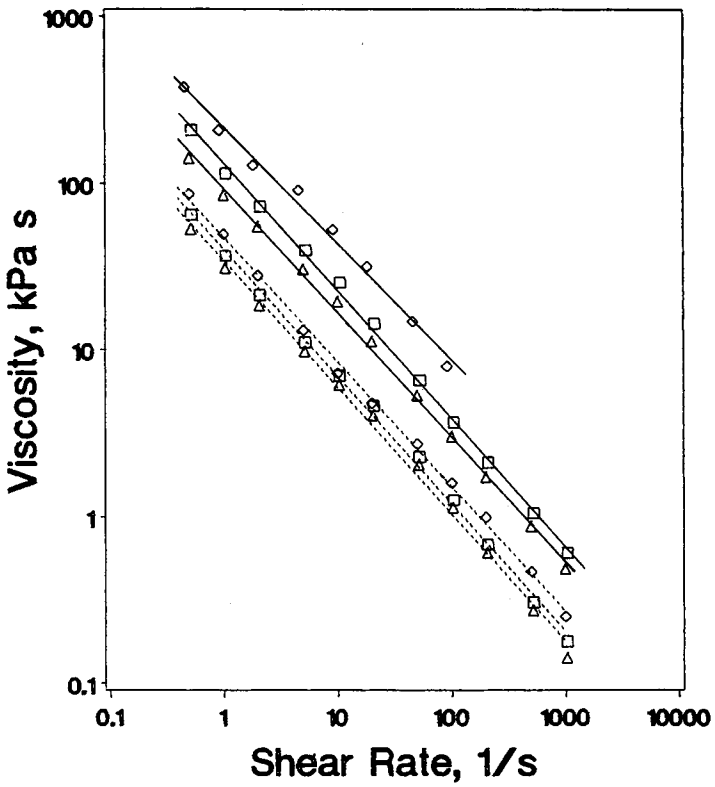

Fig. 9. Capillary rheometer flow curves of IPN of Figure 2b plasticized with various concentrations of dioctyl phthalate (DOP), at various temperatures: ◇ 0 phr; □ 8 phr; △ 16 phr; (—) 80 °C; (- - -) 150 °C.

the power law exponent remained constant. The more pronounced effect of the plasticizer on the viscosity at 80 °C, below the T_g of PS, emphasizes the important role that the more efficiently plasticized PS domains, within or between the particles, have on the flow mechanism of the elastomeric latex IPN materials. Below the T_g of PS, the plasticizer loosens the interparticle physical ties and increases the deformability of the reinforced particles, effects upon the flow that are minimized above 100 °C. Injection molding of the IPNs has demonstrated that these materials, in spite of their cross-linked nature, are processable as thermoplastics.[33]

Swelling of cross-linked polymers is used to determine their degree of cross-linking and solubility parameter δ. The swelling solvents are categorized as poorly, moderately, and highly hydrogen bonded to account for differences in their chemical character and polarity.[21] The solvent in a series of like solvents whose δ is closest to that of the polymer causes the largest volume expansion yielding the maximum swelling ratio Q_{max}, volume of solvent imbibed per unit volume of polymer. Equation (4), derived from the thermodynamics of a swollen system,[46] indicates that the solubility parameter of a polymer is the δ-axis intercept of the linear relationship between the relative

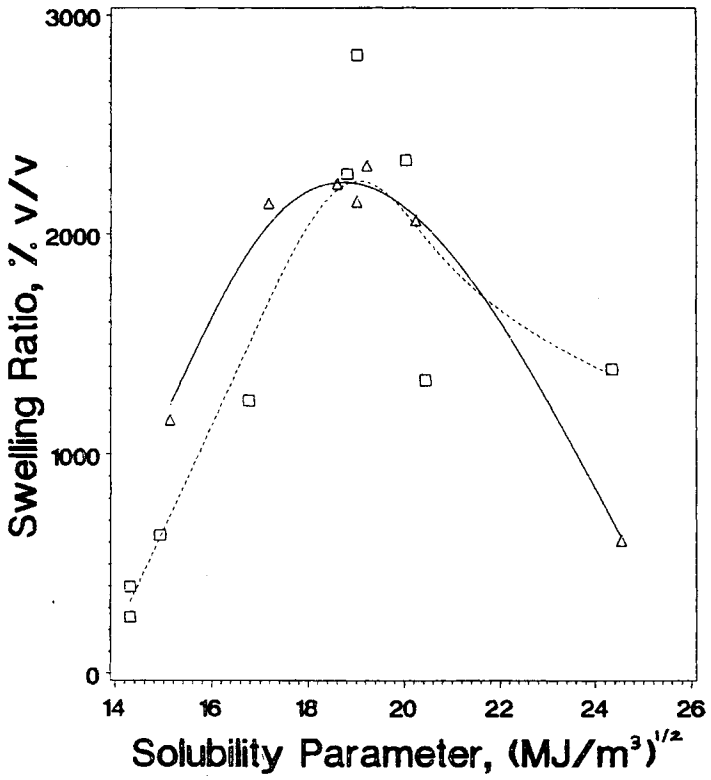

Fig. 10. Swelling ratio of latex IPN of Figure 2b with a series of pure solvents: (- - -□- - -) poorly hydrogen bonded solvents; (—△—) moderately hydrogen bonded solvents.

swelling $[(\ln(Q_{max}/Q))/v]^{1/2}$ and δ. The response of the IPN materials to immersion in a solvent yields another indication of the unique dual nature of the elastomeric latex IPN. The solubility parameters of the compression-molded latex IPN are determined in Figures 10 and 11 for a series of moderately and poorly hydrogen-bonded solvents and lie between 18.9 and 19.8 $(MJ/m^3)^{1/2}$, consistent with the solubility parameters of the homopolymers.

$$Q = Q_{max}\exp\left[-kv(\delta_p - \delta_s)\right] \tag{4}$$

where: Q = swelling ratio, volume imbibed per volume polymer
v = molar volume of solvent
δ_p = solubility parameter of the polymer
δ_s = solubility parameter of the solvent
k = constant

Since the individual particles are lightly cross-linked and the interparticle interaction is of a physical nature, one should expect a continual mass loss of polymer from the wire mesh envelope in these swelling experiments owing to the loosening of the interparticle ties and the separation of the individual submicrometer particles from the molded material. These swollen, disentangled particles, 0.2 μm in diameter, pass easily through the mesh of the metal

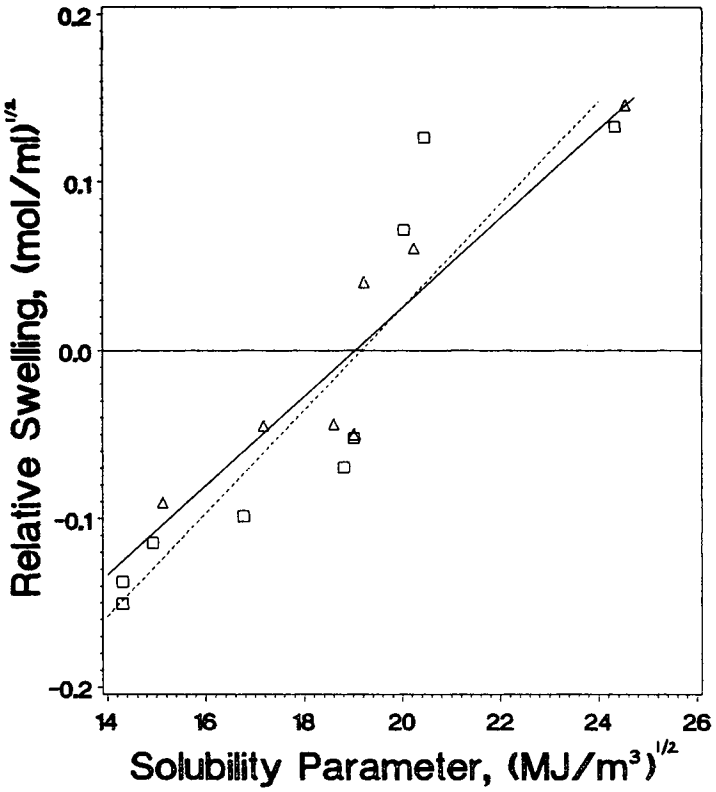

Fig. 11. Relative swelling of latex IPN of Figure 2b with series of pure solvents: (- - -□- - -) poorly hydrogen bonded solvents; (—△—) moderately hydrogen bonded solvents.

envelope, leaving new particles on the swollen sample's surface ready to disentangle in the same manner, preventing an equilibrium from being attained. In addition, removal of the highly swollen sol fraction from the lightly cross-linked IPN with time causes a decrease in the swelling ratio of the material remaining in the mesh envelope. The different maximum swelling ratios in the three curves of Figure 12 demonstrate this phenomenon in three series of experiments that were conducted in succession upon the same polymer samples with the same two solvents in different proportions.

The Microdomain Structure

Polymers that are subjected to ionizing radiation, such as γ-rays or high-energy electrons, may undergo both chain scission and cross-linking.[47,48] In some polymers, such as polyacrylates, scission dominates, but in others, such as PS, cross-linking dominates. When the polymer is embedded in an ice matrix, the difference in the behavior of the irradiated cross-linking and scission polymers is more readily apparent.[49,50] Figure 13a shows a frozen hydrated latex consisting of both pure PS and pure PMMA particles obtained by mixing the two homopolymer latices. The PMMA particles lose mass rapidly and swell, and neighboring particles fuse together. As opposed to the swelling of the PMMA particles, cavities are formed in the ice surrounding PS

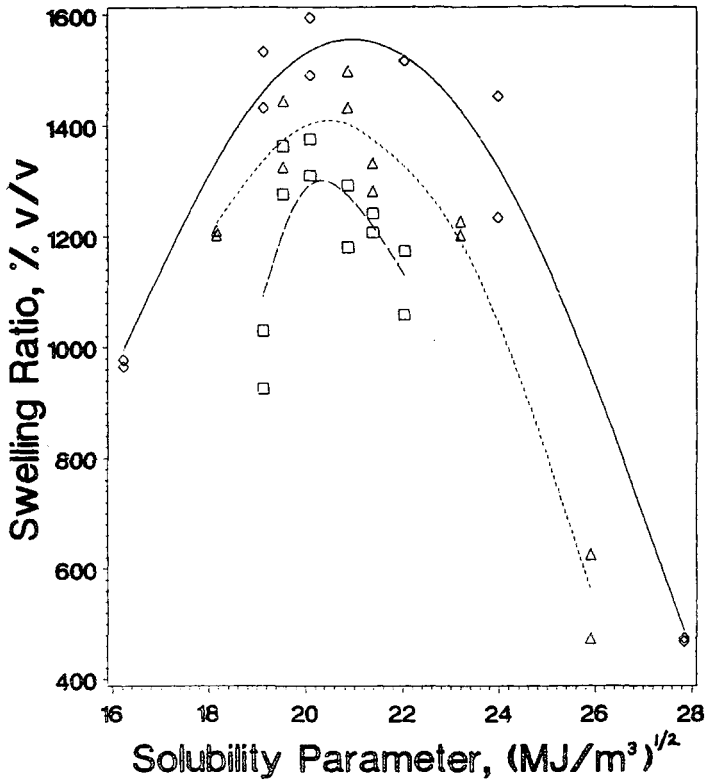

Fig. 12. Swelling of latex IPN of Figure 2b with diethyl ether and nitrobenzene mixed in various proportions: (—◇—) 24 h total immersion; (- - -△- - -) 48 h total immersion; (– –□– –) 72 h total immersion.

particles, which themselves change only little, although eventually a small decrease in diameter is observed. These differences in response to irradiation have been used to distinguish between the two types of polymer.

A schematic diagram of a hydrophobic PS seed upon which PA has been polymerized and the results of examination with cold-stage microscopy are shown in Figure 13b. There is a distinct PA shell that swells and loses mass and a distinct PS core that remains intact, consistent with the C/S structure predicted from the mechanical properties analysis. Thus the PS cores are indeed filler particles in the PA matrix, a type of structure that yields the poor tensile properties observed. On the other hand, the two-stage latex IPN from a cross-linked PA seed with 75 : 25 PA-PS in Figure 13c swells, as did the pure PA, although the swelling and mass loss for a given electron dose is less than that of a pure PA latex.[51,52] This material is composed of 25% lightly cross-linked PS that forms neither a core, nor a shell, nor individual PS homopolymer particles and therefore must be contained as an interwoven continuous network in the particle, possibly containing phase-separated microdomains, as indicated by the DSC and DMS analyses, whose size is probably of the order of only a few hundred angstroms, beyond the resolution of this technique.

(a)

(b)

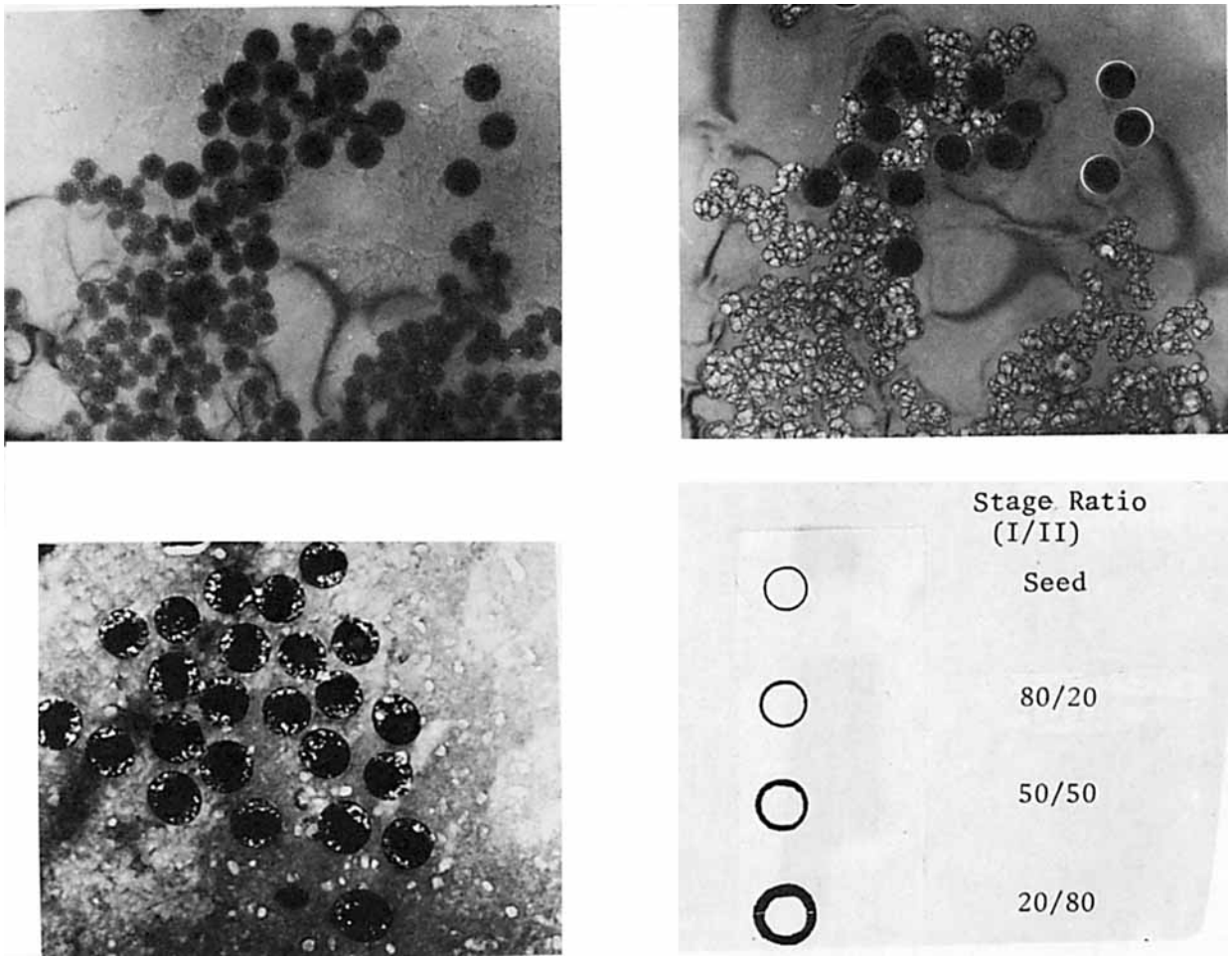

Fig. 13. Irradiation of frozen specimens of polymer latices in the TEM. (a) Mixed latices: PMMA (smaller spheres) and PS (larger spheres); left, 2 kC/m^2; right, 52 kC/m^2. (b) Two-stage latex: butyl acrylate on PS seed latex (25 : 75 PS-PBA). (c) Two-stage latex: styrene on PBA seed latex (75 : 25 PBA-PS).

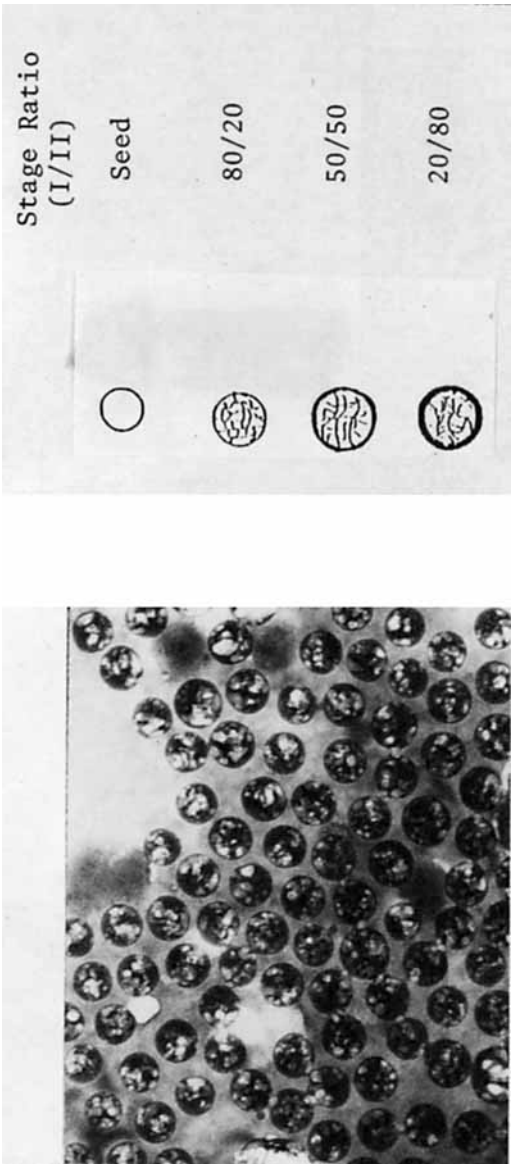

Fig. 13. *(Continued from the previous page.)*

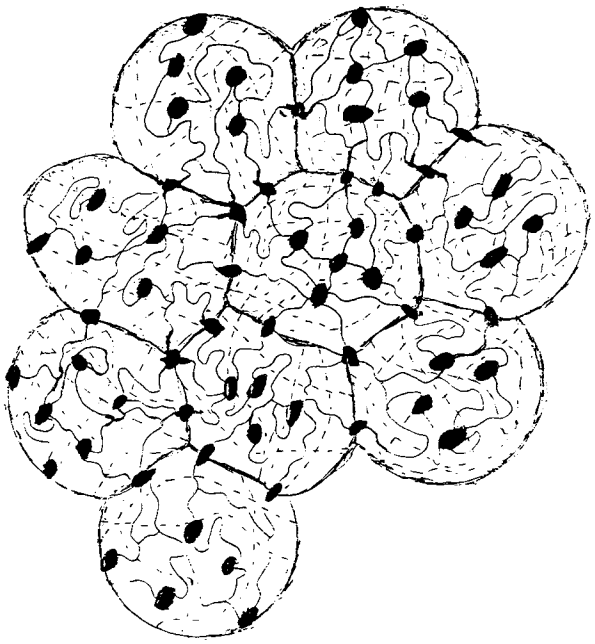

Fig. 14. Schematic cross section of molded latex IPN showing intraparticle and interparticle PS microdomains and an interwoven network structure: ● PS microdomains; (—) PS network; (- - -) PA network.

The IPN-microdomain structure, illustrated schematically in Figure 14, is consistent with the structure predicted from both the mechanical and rheological analyses. This unique multiphase particle structure results during the IPN synthesis process from the swelling of the more hydrophilic cross-linked PA seed particle by the less hydrophilic styrene monomer and its subsequent polymerization, cross-linking, and partial phase separation inside the PA network. These cross-linked elastomeric particles are reinforced by PS microdomains that increase their modulus and rigidity. Particle interconnection by rigid PS physical ties and the introduction of the strength-forming mechanism occur during the molding operation. This mechanism is operative below the T_g of PS, and at higher temperatures the system can flow under shear, in which the individually cross-linked particles constitute the flow units.

CONCLUSIONS

Latex IPNs with phase-separated microdomains can result from a two-stage emulsion polymerization procedure. The polymerization and cross-linking of the second stage (PS) upon a more hydrophilic cross-linked seed latex (PA) produces a multiphase bicontinuous structure in which the second polymer may phase separate into microdomains. Cold-stage microscopy of the IPN latex has revealed that the PS is contained within the particle, probably in an interwoven network structure whose phase-separated domain size is of the order of only a few hundred angstroms. The unique mechanical and rheological properties of the latex IPN are intimately related to its structure; the

presence of reinforcing PS intraparticle microdomains yields the high modulus, and PS interparticle ties yields the significant ultimate tensile strength. DSC and DMS studies reveal that the significant effect of plasticization upon the mechanical and rheological properties of these IPN-microdomain materials are mainly through the decrease in the T_g of the PS interparticle and intraparticle domains. Capillary rheometry indicates the existence of a stick, slip, roll flow mechanism in which the stable flow units are the cross-linked elastomeric submicrometer particles, and injection molding has shown that the latex IPN can be processed as a thermoplastic. The structure of the elastomeric latex IPN-microdomain materials results in its dual thermoset-thermoplastic nature and its unique properties.

The electron microscopy studies reported in detail in References 51 and 52 were done in collaboration with Prof. Y. Talmon of the Technion. The authors wish to thank the IMS at the University of Connecticut and the Israel Aircraft Industries for permission to use their dynamic mechanical spectrometers and Rheometrics Co. for their dynamic mechanical spectrometer studies.

References

1. D. R. Paul and S. Newman, *Polymer Blends*, Academic Press, New York, 1978.
2. J. A. Manson and L. H. Sperling, *Polymer Blends and Composites*, Plenum Press, New York, 1976.
3. L. H. Sperling, *IPNs and Related Materials*, Plenum Press, New York, 1981.
4. R. J. Williams and R. W. A. Hudson, *Polymer*, **8**, 643 (1967).
5. S. Y. Hobbs, *J. Polym. Sci., Polym. Phys. Ed.*, **16**, 1321 (1978).
6. A. J. Chompff and S. Newman, *Polymer Networks*, Plenum Press, New York, 1971, p. 435.
7. L. H. Sperling, *J. Polym. Sci., Macromol. Rev.*, **12**, 141 (1977).
8. L. H. Sperling, *Modern Plastics Int.*, **11**(10), 68 (1981).
9. J. M. Widmaier and L. H. Sperling, *Polym. Eng. Sci.*, **23**(12), 693 (1983).
10. D. I. Lee and T. Ishikawa, *J. Polym. Sci. Polym., Chem. Ed.*, **21**, 147 (1983).
11. R. A. Dickie, M. F. Cheung, and S. Newman, *J. Appl. Polym. Sci.*, **17**, 65 (1973).
12. S. Muroi, H. Hashimoto, and K. Hosoi, *J. Polym. Sci., Polym. Chem. Ed.*, **22**, 1365 (1984).
13. T. I. Min, A. Klein, M. S. El-Aasser, and J. W. Vanderhoff, *J. Polym. Sci., Polym. Chem. Ed.*, **21**, 2845 (1983).
14. D. J. Williams, *J. Polym. Sci., Polym. Chem. Ed.*, **11**, 301 (1973).
15. L. H. Sperling, *Polym. Eng. Sci.*, **24**(1), 1 (1984).
16. M. A. Winnik, *Polym. Eng. Sci.*, **24**(2), 87 (1984).
17. D. J. Hourston and R. Satgurunathan, *J. Appl. Polym. Sci.*, **29**, 2969 (1984).
18. F. A. Bovey, I. M. Kolthoff, A. I. Medalia, and E. J. Meehan, *Emulsion Polymerization*, Interscience, New York, 1955, p. 165.
19. G. Perlov, Y. Talmon, and A. H. Falls, *Ultramicroscopy*, **11**, 283 (1983).
20. L. E. Nielsen, *Mechanical Properties of Polymers and Composites*, Marcel Dekker, New York 1974.
21. J. K. Sears and J. R. Darby, *The Technology of Plasticizers*, John Wiley and Sons, New York, 1982.
22. H. Watanabe, S. Kuwahara, and T. Kotaka, *J. Rheol.*, **28**(4), 393 (1984).
23. V. M. Lobe and J. L. White, *Polym. Eng. Sci.*, **19**(9), 617 (1979).
24. H. Tanaka and J. L. White, *Polym. Eng. Sci.*, **20**(14), 949 (1980).
25. C. D. Han, *Polym. Eng. Rev.*, **1**(4), 363 (1981).
26. S. L. Rosen and F. Rodriguez, *J. Appl. Polym. Sci.*, **9**, 1601 (1965).
27. S. Montes and J. L. White, *Rubber Chem. Technol.*, **55**, 1354 (1982).
28. N. Nakajima and E. A. Collins, *J. Rheol.*, **22**(5), 547 (1978).
29. L. A. Goettler, J. R. Richwine, and F. J. Wille, *Rubber Chem. Technol.*, **55**, 1448 (1982).
30. E. A. Ekong and K. Jayaraman, *J. Rheol.*, **28**(1), 45 (1984).
31. L. L. Navickis and E. B. Bagley, *J. Rheol.*, **27**(6), 519 (1983).

32. H. Munstedt, *Polym. Eng. Sci.*, **21**(5), 273 (1979).
33. M. S. Silverstein and M. Narkis, *Polym. Eng. Sci.*, **25**(5), 257 (1985).
34. J. L. den Otter, *Plastics and Polymers*, June, 155 (1970).
35. J. M. Kenny, J. M. Castro, and N. J. Capiati, *Antec '84*, 69 (1984).
36. N. M. Bikales, *Extrusion and Other Plastics Operations*, Wiley Interscience, New York, 1971.
37. J. P. Tordella, *J. Appl. Polym. Sci.*, **7**, 215 (1963).
38. J. M. Lupton and J. W. Regester, *Polym. Eng. Sci.*, **5**, 235 (1965).
39. A. R. Berens and V. L. Folt, *Polym. Eng. Sci.*, **9**(1), 27 (1969).
40. C. L. Swanson, G. F. Fanta, and E. B. Bagley, *Polym. Compos.*, **5**(1), 52 (1984).
41. J. M. McKelvey, *Polymer Processing*, John Wiley and Sons, New York, 1962.
42. J. A. Brydson, *Flow Properties of Polymer Melts*, Iliffe Books, London, 1970.
43. F. R. Eirich, *Rheology*, Vol. II, Academic Press, New York, 1958, p. 196.
44. R. B. Bird, W. E. Stewart, and E. N. Lightfoot, *Transport Phenomena*, John Wiley and Sons, New York, 1960.
45. R. B. Taylor and A. V. Tobolsky, *J. Appl. Polym. Sci.*, **8**, 1563 (1964).
46. B. Sandholm, *Finska Kemists. Medd.*, **79**, 22 (1970).
47. F. A. Bovey, *Effects of Ionizing Radiation on Natural and Synthetic High Polymers*, Interscience Publishers, New York, 1958.
48. T. Q. Nguyen and H. H. Kausch, *J. Appl. Polym. Sci.*, **29**, 455 (1984).
49. Y. Talmon, *J. Microsc.*, **125**(2), 227 (1982).
50. Y. Talmon, *Ultramicroscopy*, **14**, 305 (1984).
51. M. Narkis, Y. Talmon, and M. S. Silverstein, *Polymer*, **26**(9), 1359 (1985).
52. Y. Talmon, M. Narkis, and M. S. Silverstein, *J. Elec. Microsc. Technique*, **2**(6), 589 (1985).

Received May 14, 1986
Accepted August 4, 1986